Mechanical Behaviour and Failure Mode of Bentheim Sandstone Under Triaxial Compression

E. Klein[1], P. Baud[1], T. Reuschlé[1] and T-f. Wong[2]

[1]Institut de Physique du Globe de Strasbourg (CNRS-ULP UMR 7516), 5, rue René Descartes, 67084 Strasbourg Cedex, France
[2]Department of Geosciences, State University of New York, Stony Brook, NY 11790-2100, U.S.A.

Abstract. Hydrostatic and triaxial compression tests have been conducted on nominally dry samples of Bentheim sandstone, a homogeneous quartz-rich sandstone with porosity of about 23%. A broad range of confining pressures were used to observe the transition from the brittle faulting to cataclastic flow regime. Mechanical data for the brittle strength and compactive yield stress can be fitted with empirical envelopes that have been shown to be applicable to other porous sandstones. However, the Bentheim sandstone is somewhat unusual in that quasi-ductile failure (characterized by an overall hardening trend punctuated by episodic strain softening and compaction band formation) was observed over a wide range of confining pressures from 120 MPa to 300 MPa. Since this failure mode is similar to observations in honeycombed cellular solids, it is speculated that the prevalence of quasi-ductile failure in the Bentheim sandstone arises from its relatively homogeneous mineralogy and grain size. Compaction band formation may be inhibited in other sandstones with higher fractions of feldspar and clay, as well as more disperse grain sizes.
© 2001 Elsevier Science Ltd. All rights reserved.

1 Introduction

The understanding of a wide range of geophysical problems requires the knowledge of the mechanical properties of rocks. An important goal of rock mechanics is to provide useful methods for predicting failure mode, mechanical strength, porosity evolution and elastic moduli. These predictions are of great importance in the oil industry, for example, where the production-induced change in reservoir fluid pressure and total stress lead to reservoir compaction and wellbore instability, each with important consequences like subsidence, seismicity and sand production (*e.g.* Martin and Serdengecti, 1984; Veeken *et al.*, 1989; Teufel *et al.*,

Correspondence to: Emmanuelle Klein
          e-mail: Emmanuelle.Klein@eost.u-strasbg.fr

1991).

The primary mechanical data are on stress as a function of strain, which is intimately related to the mode of failure. Traditionally, rock failure in compression is categorized in terms of two end members. On the one hand, a sample may show dilatancy and fail by strain softening and brittle faulting under relatively low confining pressure. On the other hand, it may show pervasive (*i.e.* delocalized) compaction and fail by strain hardening under elevated confining pressure (Paterson, 1978). At intermediate pressures, a transitional regime is sometimes observed, with failure modes involving complex localized features such as conjugate shear bands.

Recent studies have shown that the mechanical behaviour and failure mode of a porous sandstone are influenced by many competing parameters, including porosity, grain size distribution, pore fluid composition and pressure (Scott and Nielsen, 1991; Wong *et al.*, 1997; Baud *et al.*, 2000). The purpose of our work was to investigate the mechanical behaviour and failure mode of Bentheim sandstone. A series of triaxial compression tests were performed on dry samples at confining pressures ranging from 10 MPa to 350 MPa. In this paper, we present the complete set of mechanical data for hydrostatic and nonhydrostatic loadings. An intriguing feature of the Bentheim sandstone data is that over a broad range of intermediate pressures the failure mode cannot be unambiguously categorized as strictly "brittle" or "ductile". Microstructural observations of the failure modes in this transitional regime and on the mechanics of brittle-ductile transition will be discussed.

2 Experimental set-up

Bentheim sandstone occurs as welknown outcrop sandstone from the Gildehausen quarry, near the village of Bentheim (Germany). It is the same formation as the reservoir rock from the Schoonebeek oil field, a few tens of km North of the quarry. However, in terms of microstructure, petrophysical properties and composition they are very

different. The outcrop rock is very strong and quartz-rich, whereas the reservoir rock is much weaker in general and contains less quartz, and less quartz cement. Our tests have been done on the outcrop rock. It is relatively homogeneous, with mean composition of 95% quartz, 3% kaolinite, and 2% orthoclase. The quartz grains are round to sub-round, with size in the range of 50-500 μm. Most of the grains are in the size range of 200-400 μm. (Van Baaren *et al.*, 1990; Schutjens *et al.*, 1995). Cylindrical samples (20 mm in diameter, 40 mm in length) were cored out of a single block with an average porosity of ~22.8%.

Our samples were dried *in vacuo*. To circumvent the problem of breakage of strain gauges during loading, a thin layer of fast cured epoxy was first applied to fill up the surface pores before jacketing the sample with thin copper foil (of thickness 0.05 mm). The longitudinal and transverse strain gauges were then mounted in orthogonal directions on the copper jacket. The experiments at confining pressure below 100 MPa were conducted in the Strasbourg laboratory. Hydrostatic tests and triaxial tests at elevated pressures were conducted at Stony Brook. All experiments were performed at room temperature on dry samples, at a strain rate of $2.5 \cdot 10^{-5}$ s^{-1}. To measure acoustic emission (AE) activity during the triaxial experiments, we used a piezoelectric transducer on the flat surface of a steel spacer attached to the jacketed sample. The AE equipment is described in detail by Zhang *et al.* (1990). AE activity was only recorded during the tests run at Stony Brook.

3 Experimental data

In the following, we adopt the convention that compressive stresses and compactive strains are positive. The maximum and minimum (compressive) principal stresses are denoted by σ_1 and σ_3, respectively. The differential stress is denoted by $Q = \sigma_1 - \sigma_3$, and the mean stress by $P = (\sigma_1 + 2\sigma_3)/3$. Volumetric strain was calculated from the strain gauge data by summing the axial strain and twice the transverse strain.

3.1 Deformation under hydrostatic loading

Figure 1 compiles data for five hydrostatic tests. At relatively low pressure, the response of the rock is highly non-linear. At elevated pressure, the volumetric strain data display reasonable reproducibility. The critical pressure P^* for the onset of grain crushing and pore collapse in a porous sandstone is commonly characterized by an accelerated decrease of volume and a surge in AE activity (Zhang *et al.*, 1990; Brace, 1978). As shown in Fig.1, a drastic increase in AE activity occurs at ~390 MPa. This increase corresponds to a subtle inflection of the stress-strain curve (marked as P^*). Microstructural observations of deformed samples confirm the onset of grain crushing and pore collapse beyond this pressure, whereas a sample deformed to 375 MPa appears relatively undamaged. Moreover, a somewhat unusual feature in the Bentheim sandstone is a precursory surge of AE activity at ~210 MPa, which is about half of

the critical pressure P^* (Fig.1).
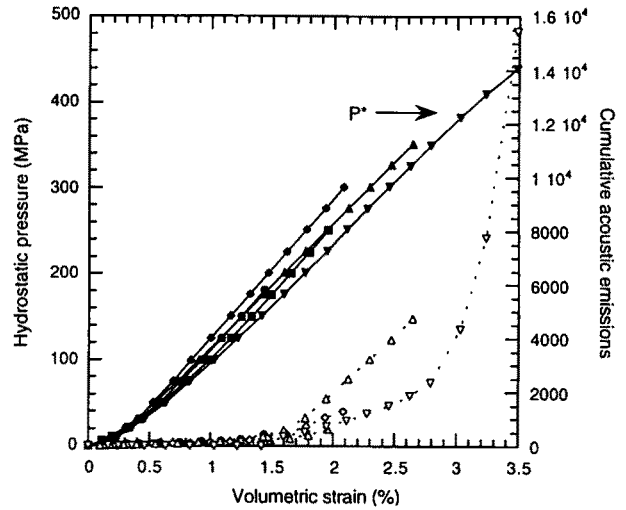
Fig. 1. Hydrostatic pressure (solid curve) and cumulative acoustic emissions (dotted curve) versus volumetric strain for five hydrostatic tests on Bentheim sandstone. P^* is the critical pressure for the onset of grain crushing and pore collapse.

3.2 Triaxial compression: the brittle regime

Under triaxial loading, the failure mode of Bentheim sandstone is characterized by a typical Mohr-Coulomb brittle deformation regime at confining pressures up to 60 MPa (Fig.2). The differential stress attains a peak beyond which strain softening occurs, accompanied by a rapid stress drop to a residual level (Fig.2a). The peak stress increases with confining pressure, which is typical of Mohr-Coulomb type of brittle failure (Paterson, 1978). The volume initially decreases probably due to crack closure and elastic grain contact deformation, but near the peak stress it reverses to an increase indicating the inception of dilatancy (Fig.2b). Visual inspection of these samples confirmed that each had failed by shear localization along an inclined macroscopic shear band cutting across each sample.
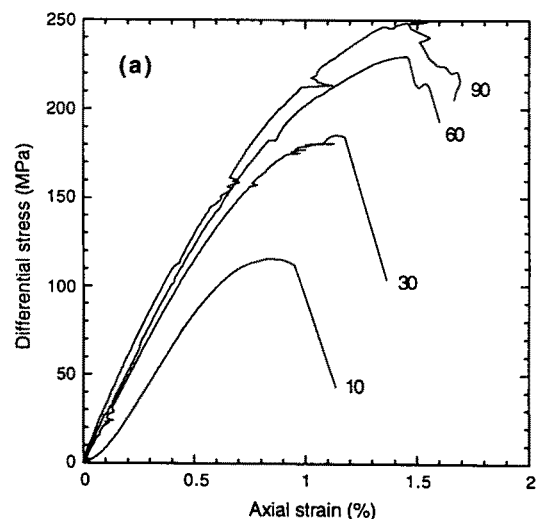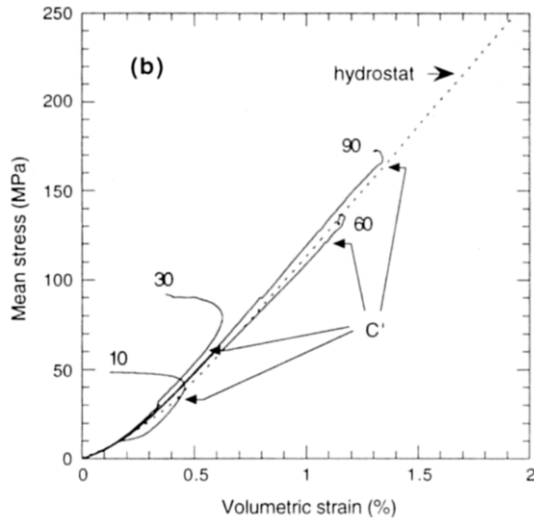
Fig. 2. (a) Differential stress versus axial strain; and (b) mean stress $(\sigma_1+2\sigma_3)/3$ versus volumetric strain for Bentheim sandstone under triaxial tests at low confining pressures (labelled in MPa near the end of each curve). The dotted line corresponds to the reference hydrostatic curve. *C'* corresponds to the stress at the onset of dilatancy.
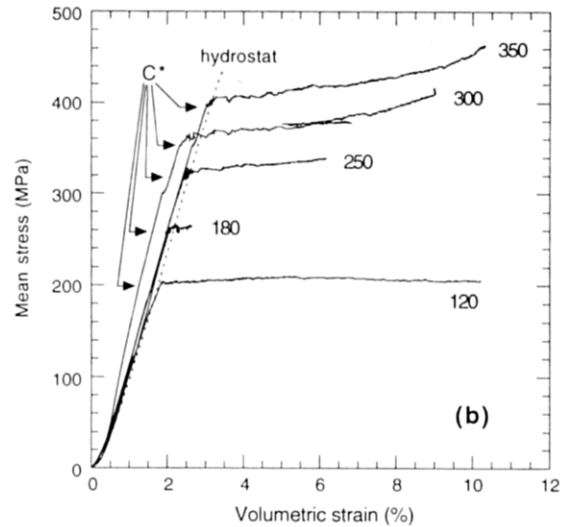
Fig. 3. (a) Differential stress (solid curve) and cumulative acoustic emissions (dotted curve) versus axial strain; and (b) mean stress $(\sigma_1+2\sigma_3)/3$ versus volumetric strain for Bentheim sandstone under triaxial tests at elevated confining pressures (labelled in MPa on each figure). The dotted line in Fig. 3b corresponds to the reference hydrostatic curve. *C** corresponds to the stress at the onset of shear-enhanced compaction.

3.3 The transitional regime: quasi-brittle and quasi-ductile failures

Over a relatively broad range of confining pressure (90 - 300 MPa), the mechanical behaviour and failure mode of our samples cannot be definitively identified as in the "brittle" or "ductile" regime. While the sample deformed at 90 MPa pressure attained a peak stress and showed strain softening (Fig.2a), dilatancy was negligible (Fig.2b) and the cylindrical surface of the failure sample is marked by several conjugate shears instead of a single shear band. We will refer to this transitional failure mode as "quasi-brittle".

In contrast, deformation at pressures ranging from 120 MPa to 300 MPa was characterized by "ductile" attributes, with an overall strain hardening trend (Fig.3a) and shear-enhanced compaction (Curran and Carroll, 1979).

The latter is defined by an accelerated decrease in porosity in comparison to the hydrostat beyond a critical stress state (indicated by *C** in Fig.3b)

However, the failure in the Bentheim sandstone is different in two important aspects from ductile failure in other porous sandstones previously studied (Wong *et al.*, 1997; Wu *et al.*, 2000). First, while a sample undergoes shear compaction, the overall hardening trend is punctuated by episodic softening with stress drops up to 30 MPa (Fig.3a).
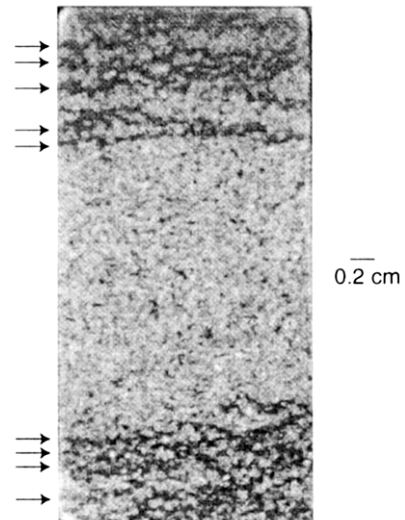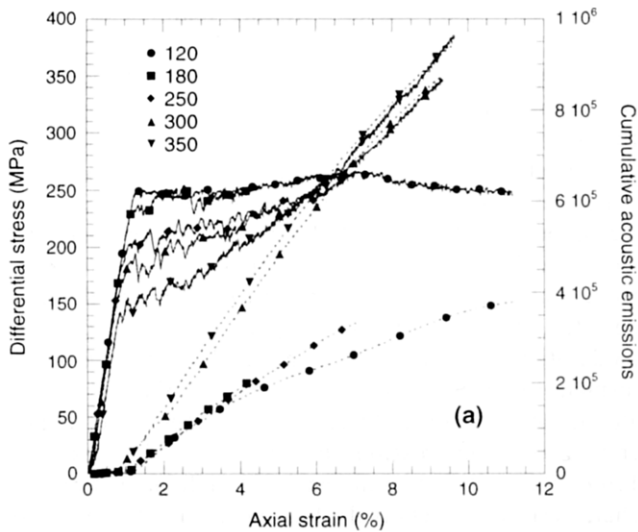
Fig. 4. General view of the thin section of the sample deformed at 300 MPa confining pressure. Note the compaction bands (black zones indicated by the arrows) perpendicular to maximum compressive stress (oriented in an axial direction). The gray areas correspond to quite undisturbed material.

Second, microstructural observations indicate that damage in these failed samples can be highly localised. In the thin

section of a sample deformed at 300 MPa confining pressure, several "compaction bands" subperpendicular to σ_1 (Mollema and Antonellini, 1996; Olsson, 1999) were evident (Fig.4). These bands tend to cluster near the upper and lower ends of a failed sample, and separating them are zones with relatively little damage. Microstructural analysis indicates that the porosity in the bands is only a few percent compared with the 16 to 23% porosity in the less damaged zones We will refer to this transitional failure mode as "quasi-ductile".

3.4 Envelopes for brittle strength and compactive yield

For samples in the brittle and quasi-brittle regimes, we determined the peak stress and C', stress at the onset of dilatancy (Fig.2). These critical stresses show a positive pressure dependence, and the peak stress data fit a parabolic envelope of the form (Khan *et al.*, 1991; Wong *et al.*, 1997) (Fig.5):

$$\frac{Q}{P*} - q_0 = -m\left(\frac{P}{P*} - p_0\right)^2 \qquad (1)$$

with $(p_0, q_0) = (0.49, 0.62)$ and $m = q_0 / (1 - p_0)^2$.

At elevated pressures (120 - 350 MPa), the compactive yield stresses $C*$ (Fig.3b) for the onset of shear-enhanced compaction show a negative pressure dependence, and data map out an elliptical cap of the form (Wong *et al.*, 1997) (Fig.5):

$$\frac{\left(\frac{P}{P*} - \gamma\right)^2}{(1 - \gamma)^2} + \frac{\left(\frac{Q}{P*}\right)^2}{\delta^2} = 1 \qquad (2)$$

with the grain crushing pressure $P* = 390$ MPa, and parameter values $\gamma = 0.61$ and $\delta = 0.6$ that fit the Bentheim sandstone data.

4 Discussion

In this study, we investigated the mechanical behaviour of Bentheim sandstone under triaxial compression, at a pressure range wide enough to observe both brittle and ductile failure. Our data for the brittle strength and compactive yield stress can be fitted with empirical envelopes that have been shown to be applicable to other porous sandstones (Wong *et al.*, 1997; Baud *et al.*, 2000). However, the Bentheim sandstone is somewhat unusual in that quasi-ductile failure (characterized by episodic strain softening and development of compaction bands) was observed over a wide range of pressures from 120 MPa to 300 MPa. Although inspection of the exterior of the sample that failed at 350 MPa did not reveal evident localized bands, the overall hardening trend was punctuated by at least four relatively sharp stress drops (Fig.3a). Acoustic emissions tend to increase sharply at the onset of shear-

enhanced compaction (Fig. 3a) but there is no obvious relationship between stress drops and sudden local increase of acoustic emissions due to their overall high level of occurrence. There seems to be a correlation between the number of stress drops and the number of compaction bands. Moreover, the number of compaction bands increases and they propagate from the ends of the sample towards its centre as the axial strain is increased. However, in the absence of more detailed microstructural observations we cannot categorically identify the failure mode of this sample as fully "ductile" or "quasi-ductile".
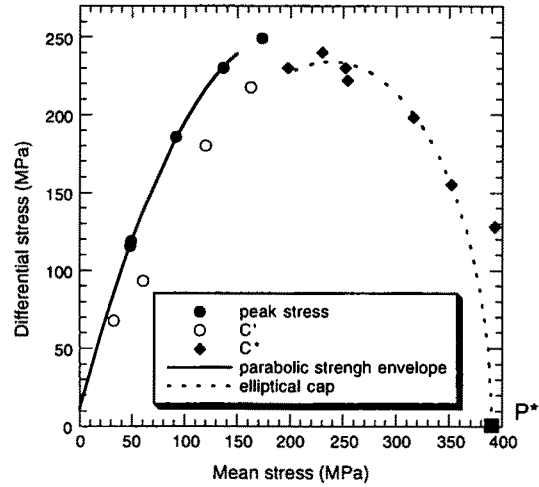
Fig. 5. The brittle strength (solid circles), critical stress C' at the onset of dilatancy (open circles), and compactive yield stress $C*$ at the onset of shear-enhanced compaction (solid diamonds) of Bentheim sandstone. The parabolic strength envelop (Eq.(1)) and elliptical cap (Eq.(2)) that fit our data are shown as solid and dotted curves, respectively. $P*$ is the critical pressure for the onset of grain crushing and pore collapse.

The formation of compaction bands seems to be an intrinsic failure mode in the quasi-ductile regime and not due to some experimental artefacts. We observed similar localisation features in samples deformed in two different machines (in Stony Brook and Strasbourg), and in duplicate tests with and without lubrication at the interface between sample and steel spacer. Similar features were also observed in a nominally dry sample deformed at a slower strain rate of $1.3 \cdot 10^{-5}$ s^{-1} and in a saturated sample deformed at confining pressure of 250 MPa and pore pressure of 10 MPa.

Compaction bands were first documented in aoelian sandstone formation (Mollema and Antonellini, 1996), and recent theoretical analyses (Olsson, 1999) have clarified the mechanical conditions under which such a localisation mode may develop. It is of interest to note that the quasi-ductile attributes (with an overall hardening trend modulated by strain softening and compaction band formation) observed here are very similar to data for aluminium and polycarbonate honeycombs under uniaxial and biaxial compression (Papka and Kyriakides, 1998; 1999). Since such two-dimensional cellular materials are characterized by relatively homogeneous structures, one may speculate that the prevalence of quasi-ductile failure in

the Bentheim sandstone also arises from its relatively homogeneous mineralogy and grain size. Such a quasi-ductile failure mode may be inhibited in other sandstones with higher fractions of feldspar and clay, as well as more disperse grain sizes. Elucidation of this question is central to a fundamental understanding of the brittle-ductile transition, and future studies on various sandstones will explore this question in a more comprehensive manner.

References

Baud, P., Zhu, W., and Wong, T.-f., Failure mode and weakening effect of water on sandstone, *J. Geophys. Res.*, 2000, in press.

Brace, W.F., Volume changes during fracture and frictional sliding: a review, *Pure Appl. Geophys.*, *166*, 603-614, 1978.

Curran, J.H. and Carroll, M.M., Shear stress enhancement of void compaction, *J. Geophys. Res.*, *84*, 1105-1112, 1979.

Khan, A.S., Xiang, Y., and Huang, S., Behavior of Berea sandstone under confining pressure, part I: Yield and failure surfaces, and nonlinear elastic response, *Int. J. Plasticity*, *7*, 607-624, 1991.

Martin, J.C. and Serdengecti, S., Subsidence over oil and gas fields, *Geol. Soc. Am. Rev. Eng. Geol.*, *6*, 23-24, 1984.

Mollema, P.N. and Antonellini, M.A., Compaction bands: a structural analog for anti-mode I cracks in aeolian sandstone, *Tectonophysics*, *267*, 209-228, 1996.

Olsson, W.A., Theoretical and experimental investigation of compaction bands in porous rock, *J. Geophys. Res.*, *104*, 7219-7228, 1999.

Papka, S.D. and Kyriakides, S., In-plane crushing of a polycarbonate honeycomb, *Int. J. Solids Struct.*, *35*, 239-267, 1998.

Papka, S.D. and Kyriakides, S., Biaxial crushing of honeycombs - Part I: Experiments, *Int. J. Solids Struct.*, *36*, 4367-4396, 1999.

Paterson, M.S., Experimental deformation – The Brittle Field, 254 pp., Spinger-Verlag, New-York, 1978.

Schutjens, P.M.T.M., Hausenblas, M., Dijkshoorn, M., and Van Munster, J.G., The influence of intergranular microcracks on the petrophysical properties of sandstone - experiments to quantify effects of core damage, *Proceeding of International Society of the Society of Core Analysts*, 1995.

Scott, T.E. and Nielsen, K.C., The effects of porosity on the brittle-ductile transition in sandstones, *J. Geophys. Res.*, *96*, 405-414, 1991.

Teufel, L.W., Rhett D.W., and Farrell, H.E., Effect of reservoir depletion and pore pressure drawdown on in situ stress and deformation in the Ekofish field, North Sea, *Proc. U.S. Rock Mech. Symp.*, *32*, 63-72, 1991.

Van Baaren, J.P., Vos, M.W., and Heller, H.K.J., Selection of outcrop samples, Dietz Laboratory report, Delft University, 1990.

Veeken, C.A.M., Walters, J.V., Kenter, C.J, and Davis, D.R., Use of plasticity models for predicting borehole stability, in Rocks at Great Depth, 2, eds. Maury, V. and Fourmaintaux, D., 835-844, 1989.

Wong, T.-f., David, C., and Zhu, W., The transition from brittle faulting to cataclastic flow in porous sandstones: mechanical deformation, *J. Geophys. Res.*, *102*, 3009-3025, 1997.

Wu, X.Y., Baud, P., and Wong, T.-f., Micromechanics of compressive failure and spatial evolution of anisotropic damage in Darley Dale sandstone, *Int. J. Rock Mech. Min. Sci.*, *37*, 143-160, 2000.

Zhang, J., Wong, T.-f, and Davis, D.M., High pressure embrittlement and shear-enhanced compaction in Berea sandstone: acoustic emission measurement and microstructural observation, *Rock Mechanics Contributions and Challenges, Proceedings of 31st U.S. Symposium on Rock Mechanics*, A. A. Balkema, Rotterdam, Netherlands, 653-660, 1990.